Numerical Study on Smoke Temperature in Underground Plant of Hydropower Station

Chang Liu*, Binbin Zhao, Kunpeng Ji, Jingshan Han, Yi Liu

China Electric Power Research Institute, Beijing, 100192, China

*Corresponding author's e-mail:253065625@qq.com

Abstract. Hydropower stations, as critical infrastructure for national development in China, play an essential role in electricity supply. Meanwhile, a large number of underground caverns are constructed with large fire risk threatening personnel safety. Numerical simulations on fire scenarios in hydropower stations were conducted in this study, considering fire source power, smoke exhaust volume, and fire source location. The maximum smoke temperature rise, the smoke layer height, and the vertical temperature rise of the fire source center in underground plant were analyzed. Results indicated that an increase in fire source power has a significant impact on the maximum ceiling temperature rise, and vertical temperature rise of the fire source center. In contrast, an increase in smoke exhaust rate has a smaller impact, only affecting them under conditions of high fire source power. Regarding the smoke layer height, the results showed that the influence of fire source power, smoke exhaust volume, and fire source locations was relatively small. Through a comparison of fire in the middle and at the end of the plant, it was discovered that the fire hazard under the latter location was significantly greater than that under the former location. By analyzing the smoke behavior characteristics in large space underground plant of hydropower station, this study provides a theoretical basis for adopting prevention and response measures to support fire safety in underground plant of hydropower stations.

Keywords: hydropower station; numerical simulation; smoke temperature; smoke layer height; vertical temperature rise.

1 Introduction

In recent years, China's hydropower engineering has been developed rapidly to support the electrical power and clean energy demand, and the number of large hydropower stations has been gradually increased. Hydroelectric power station provides us with the convenience of electricity, but also brings about fire safety concern in underground space. When a fire occurs in a hydropower plant, it produces a large amount of toxic and harmful gases, and at the same time produces high-temperature smoke, which makes it difficult for firefighters to extinguish and rescue. Due to the large space of the

P. Liu et al. (eds.), *Proceedings of the 2024 5th International Conference on Civil, Architecture and Disaster Prevention and Control (CADPC 2024)*, Atlantis Highlights in Engineering 31,
https://doi.org/10.2991/978-94-6463-435-8_20

spreading to both ends of the plant will settle rapidly and fill the whole space, and on-site personnel at operation platform with different heights faces serious evacuation difficult. Therefore, it is highly essential to pay attention to the fire safety in underground plant of hydropower station.

Smoke temperature is an important parameter to evaluate the spread and settlement process. Zhang Huanhuan[1] conducted 1:10 scale experiments to study the dispersion of temperature of smoke near the ceiling in tunnel fires under different fire source power, fire source location, and smoke extraction rates. The maximum thermal plume temperature of the ceiling jet was predicted by Alpert[2] using an empirical formula. Smoke diffusion and temperature variations in comprehensive cable tunnel fires were investigated by Li Wenting[3] through numerical simulations using numerical simulation software. A numerical model that closely resembles actual tunnels was established by W. K. Show[4] using CFAST software to analyze the smoke characteristics during tunnel fires. Simulation analysis was conducted by Liu Zhenyu[5] using numerical simulation software to study the influence of fire source height on the spreading behavior of tunnel smoke in the case of dual fire sources. Xu Chenggang[6] established a longitudinal attenuation model of smoke temperature in dual fire source tunnel fires under natural ventilation conditions through small-scale similarity experiments. A series of full-scale numerical simulations were conducted by Ren F[7] to study the development of temperature patterns along a longitudinal axis and the maximum temperature increase in subway tunnels under the condition of dual fire sources. The influence of aspect ratio, longitudinal ventilation velocity, and fire heat release rate on the lateral and longitudinal attenuation characteristics of smoke temperature in tunnel fires was studied by Zhang[8] through scaled model experiments and CFD simulations. Xu Chenggang[9] found that under natural ventilation conditions, the smoke temperature of a double fire source tunnel fire decreases exponentially along the length direction. Temperature distribution characteristics of fire smoke in train carriages under different fire source powers and positions in natural ventilation tunnels were studied by Cong Wei[10]. Zhong Wei[11] compared the smoke exhaust effects of ceiling mechanical smoke exhaust and lateral mechanical smoke exhaust in tunnel fires through numerical simulation.

In summary, extensive simulation and experimental research has been conducted by scholars domestically and internationally to investigate the structural characteristics of narrow and confined spaces. The current research focuses on the longitudinal attenuation of ceiling smoke temperature, the lateral distribution of fire temperatures in tunnels, and the dimensionless heat release rate. However, there is limited research on smoke characteristics in long and narrow plant with large space. Therefore, the main objective of this paper is to study the smoke characteristics of underground plant in hydropower stations by fire simulation. The results of this study could provide references for fire prevention and risk evaluation.

2 Numerical simulation model construction

Due to the challenges associated with conducting high power fire experiments, numerical simulation methods were chosen for our research. Numerical simulation allows us to more easily control the power of the fire source and the volume of smoke exhaust, offering advantages over experimental methods in terms of reproducibility and cost-effectiveness. Additionally, potential hazards present in experimental setups could be avoided with numerical simulation. As shown in Figure 1, the simulated model represents a large underground plant, with maximum spatial dimensions of 438 m in length, 30 m in width, and 74 m in height[12]. The cross-sectional shape of the factory is rectangular, and it is equipped with two smoke exhaust outlets at the top for ventilation control using mechanical smoke extraction. Thermocouples were placed beneath the ceiling to measure the temperature recorded in the hot smoke layer. Measurement points for the smoke layer were distributed within the underground space to determine the thickness of the hot smoke layer. Furthermore, thermocouple trees were positioned above the fire source to measure the vertical temperature rise. Based on previous studies[13], the power of fire sources in underground spaces of hydropower stations could reach several tens of megawatts. Therefore, fire power was set at 40 MW, 60 MW, and 80 MW, with fire sources located at two different positions. The hydropower station was modeled as a concrete structure, and n-heptane was designated as the fuel based on the actual construction materials used. The smoke exhaust rates of the two outlets at the top were set at 40 m^3/s, 50 m^3/s, and 60 m^3/s, resulting in a total of 18 simulation cases. The simulation cases are presented in Table 1.

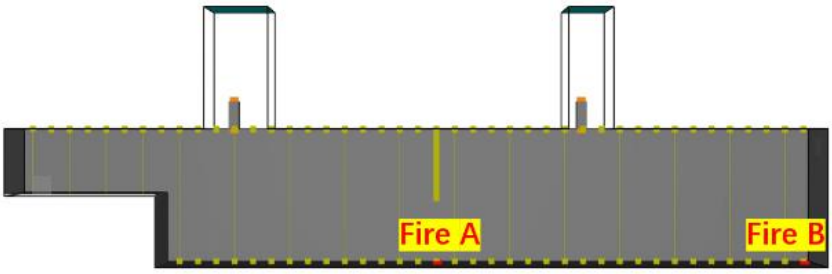

Fig. 1. The numerical simulation model

Table 1. Fire simulation cases

Simulation case	fire source location	Fire source power MW	Smoke exhaust air volume m^3/s
1	A	40	40
2	A	60	40
3	A	80	40
4	B	40	40
5	B	60	40

6	B	80	40
7	A	40	50
8	A	60	50
9	A	80	50
10	B	40	50
11	B	60	50
12	B	80	50
13	A	40	60
14	A	60	60
15	A	80	60
16	B	40	60
17	B	60	60
18	B	80	60

The grid scale is a vital role that determines the precision of numerical simulation calculations. In general, a finer grid can assure higher precision of the numerical simulation outcome. However, excessively fine grids may introduce errors in the computed results and prolong the simulation time. Therefore, the selection of the grid size is of great importance. Eq.(1) is commonly used to calculate the flame characteristic diameter D^*[14]:

$$D^* = \left(\frac{\dot{Q}}{\rho_\infty c_p T_\infty \sqrt{g}}\right)^{0.4} \tag{1}$$

Let δ_x represent the grid size. According to previous research recommendations, the optimal range for the ratio D^*/δ_x is suggested to be between 4 and 16. By substituting the minimum heat release rate set within this research into the equation above, the approximate range of the grid scale may be estimated as around 0.4 m to 1.3 m. Taking into account both the level of simulation detail and computation time, a grid size of 1 m × 1 m × 1 m is chosen in this study.

3 Maximum temperature rise of the roof smoke layer

According to Figure 2, the variation of the vertical temperature rise of the ceiling at different operating conditions for the fire source point A is observed. As we move away from the center of the fire source, the maximum ceiling temperature rise is decreased at both ends of the fire source. Meanwhile, the maximum temperature rise directly above the fire source point reaches its peak value, and the maximum temperature rise at the ends of the fire source exhibits a symmetric shape. The most significant variation of the maximum temperature rise of the smoke layer is observed directly above the fire source, and it decreases as the distance from the fire source is increased. For example, the highest temperature increase directly over the fire point can reach up to 110°C. Nevertheless, once the distance away from the fire hits 100 meters, the temperature fluctuation is minimal, and the highest temperature increase is only 70°C.

Under the same smoke exhaust volume conditions, the maximum temperature rise of the ceiling is significantly impacted by the change in fire source power. Taking the

40 m^3/s smoke exhaust volume condition as an example, when the fire source power is 40 MW, the maximum temperature rise of the ceiling is 66°C; when the fire source power increases to 60 MW, the maximum temperature rise of the ceiling rises to 88°C; and as the power of the flame origin increases to 80 MW, the highest temperature increase of the ceiling reaches its maximum value of 105°C. Under the 50 m^3/s smoke exhaust volume condition, as the power of the flame origin increases to 40 MW, the highest temperature increase of the ceiling reaches 67°C; as the power of the flame origin increases to 60 MW, the highest temperature increase of the ceiling rises to 84°C; and as the power of the flame origin increases to 80 MW, the highest temperature increase of the ceiling reaches its maximum value of 104°C. Under the 60 m^3/s smoke exhaust volume condition, as the power of the flame origin increases to 40 MW, the highest temperature increase of the ceiling reaches 65°C; as the power of the flame origin increases to 60 MW, the highest temperature increase of the ceiling rises to 90°C; and as the power of the flame origin increases to 80 MW, the highest temperature increase of the ceiling reaches its maximum value of 108°C.

The variation in the highest temperature increase of the ceiling under different fire source power conditions, can be explained as follows: as the fire source power is increased, the heat release rate per unit time increases, resulting in increasing the thermal radiation and convective heat received by the smoke layer in the space. Therefore, the highest temperature increase of the ceiling with the increase in fire source power. Furthermore, under the same fire source power, the variation in the maximum temperature rise of the ceiling under different smoke exhaust volume conditions can be explained as follows: an increase in smoke exhaust volume implies an increase in the quantity of smoke discharged per unit time. However, due to the larger amount of smoke generated, the thickness of the smoke layer in the entire space continues to increase. Although a portion of the smoke is exhausted, heat continues to accumulate, leading to a continuous increase in the temperature of the smoke layer. Therefore, as the volume of smoke exhaust grows, the decrease in the highest temperature increase of the ceiling is relatively small. In summary, the highest temperature increase of the ceiling increases with the increase in fire source power under the same smoke exhaust volume, and reduces with the rise in smoke exhaust volume under the same heat source intensity, although the variation is small.

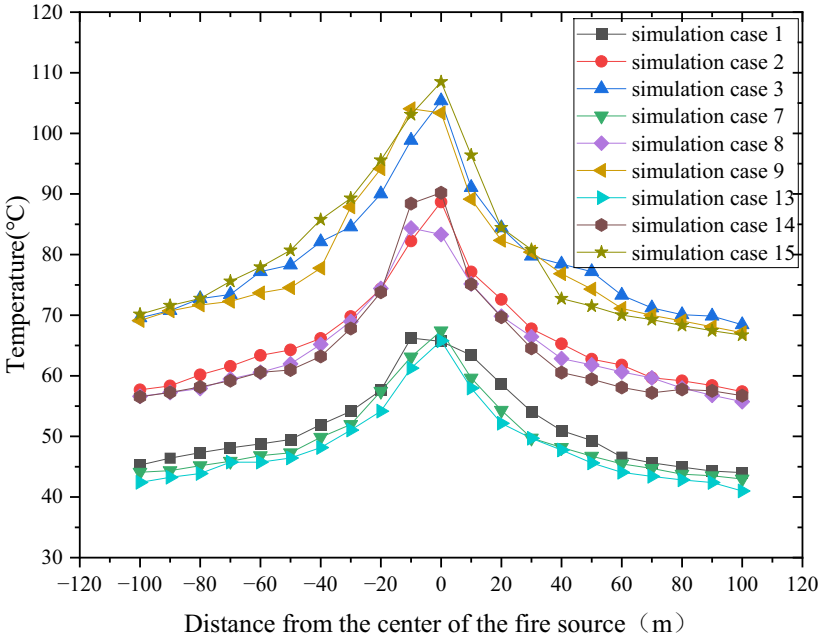

Fig. 2. Longitudinal temperature rise of ceiling under different simulation cases at ignition point A

The longitudinal temperature rise of the ceiling under different operating conditions of fire source point B is depicted in Figure 3. From the figure, it can be observed that as the distance from the center of the fire source increases, the overall trend of the maximum longitudinal temperature rise of the ceiling decreases. The maximum temperature increase of the ceiling occurs directly above the fire source point, and reaches its maximum value. Located 410 m away from the center of the fire source, the minimum value of the highest temperature increase of the ceiling is reached. Under the condition of a smoke exhaust volume of 40 m^3/s and a fire source power of 40 MW, the highest temperature increase of the ceiling reaches 72℃. As the power of the flame origin increases to 60 MW, the maximum temperature rise of the ceiling rises to 95℃. As the power of the flame origin increases to 80 MW, the highest temperature increase of the ceiling reaches its maximum value of 109℃. Under the conditions of a smoke exhaust volume of 50 m^3/s and 60 m^3/s, the highest temperature increase of the ceiling under different fire source power conditions exhibits a similar pattern to that under the condition of a smoke exhaust volume of 40 m^3/s, with a small variation. Furthermore, under the conditions of two different fire source positions, A and B, the highest temperature increase of the ceiling under the fire origin position B is marginally greater than that under the fire origin position A, but the difference is not significant. This indicates that different ignition points have a relatively small impact on the maximum temperature rise of the ceiling.

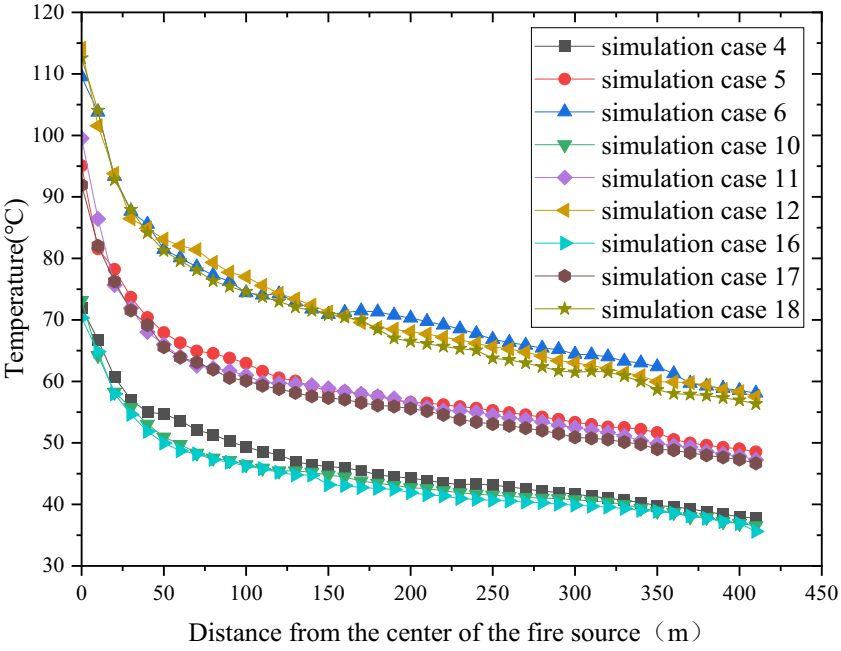

Fig. 3. Longitudinal temperature rise of ceiling under different simulation cases at ignition point B

4 Analysis of smoke layer height

The change in smoke layer height over time under varying operational conditions is illustrated in Figure 4. Analyzing the condition of fire source point A, it is observed that the smoke layer height exhibits an overall decreasing trend over time. Prior to 200 s, a relatively steep slope in the change of smoke layer height is noted, indicating a significant variation during this stage. By the 400 s mark, the smoke layer height has already decreased to 20 m. As time progresses beyond 400 s, the change in smoke layer height slows down noticeably, but it continues to decrease. At the 900 s mark, the smoke layer height reaches approximately 12 m. After 900 s, the smoke layer height remains almost constant. This might be explained by the slow decline in heat release rate and smoke generation rate during the fire process. This equilibrium between smoke generation and emission with the external environment leads to the relatively stable smoke layer height.

When considering the operational state of fire source point A, the smoke layer height images under different exhaust gas flow rates of 40 MW can be observed from Figure 4(a). Evidently, the height of the smoke layer is at its lowest value under the exhaust gas flow rate of 40 m^3/s. A marginal rise in the height of the smoke layer is observed under the exhaust gas flow rate of 50 m^3/s compared to the 40 m^3/s condition, and a slightly higher value is noted under the exhaust gas flow rate of 60 m^3/s compared to the 50 m^3/s condition. In other words, under the same fire source power, the height of

the smoke layer slightly rises as the rise in exhaust gas flow rate, but the overall increase is relatively small. From Figure 4(b), the smoke layer height images under different fire source powers of 40 m^3/s can be observed. Evidently, the fire source power increases, the smoke layer height decreases overall. Before 260 s, the difference in smoke layer height is significant, reaching up to 10 m. As time progresses, the difference in smoke layer height gradually decreases and reaches approximately 2 m at the final moment.

Under different operating conditions at fire source point B, it is noticeable from Figure 4(c) and (d) that the trend of smoke layer height with time is similar to that of fire source point A, showing an overall decreasing trend with small differences. For fire source point B, the smoke layer height has a steeper slope and decreases rapidly to around 18 m at 320 s. Subsequently, a slight increase is followed by a gradual decrease to the lowest point after 460 s. In summary, under the same fire source power condition, increasing the exhaust gas flow rate can slightly increase the smoke layer height, but the increase is small. On the other hand, under the same exhaust gas flow rate condition, increasing the fire source power can significantly reduce the smoke layer height during the initial phase of the fire. In the ultimate phase of the fire, the difference in smoke layer height is small.

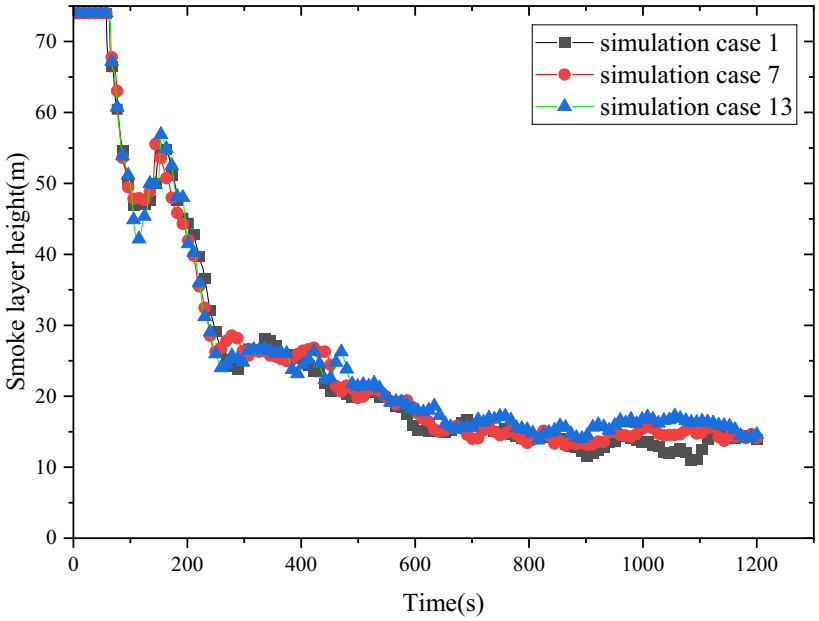

(a) A fire source point with 40 MW fire source power

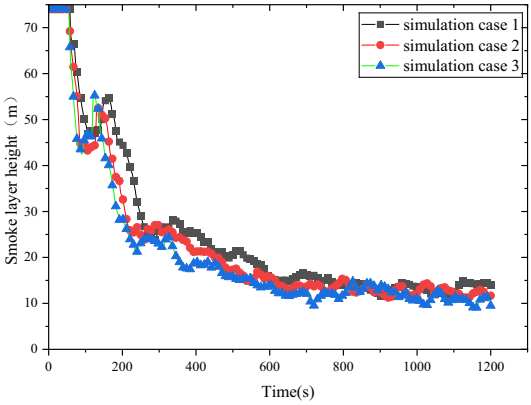

(b) A fire source point with 40 m3/s smoke exhaust volume

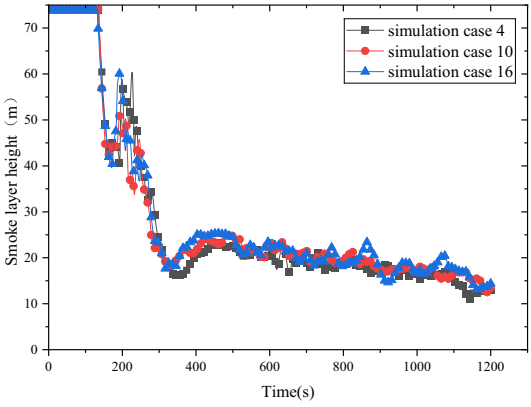

(c) B fire source point with 40 MW fire source power

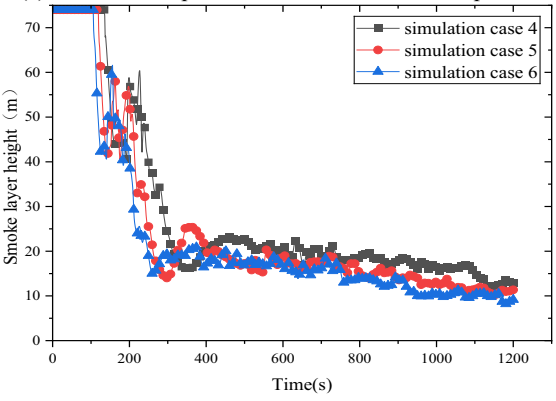

(d) B fire source point with 40 m3/s smoke exhaust volume

Fig. 4. Changes in smoke layer height over time under different simulation cases

5 Vertical temperature rise at the center of the fire source

From the observation of the vertical temperature rise on the roof at fire source point A in Figure 5, it can be seen that the temperature decreases exponentially with increasing vertical distance from the fire source center[15], reaching its minimum at the highest point. Under the same exhaust gas flow rate condition, the vertical temperature rise at the fire source center is significantly influenced by the change in fire source power. For instance, under the condition of an exhaust gas flow rate of 40 m^3/s, with the fire source power of 40 MW, the highest temperature in the vertical direction is 107°C at 35 m away from the fire, and 65°C at 72 m away from the fire. When the fire source power increases to 60 MW, the highest temperature in the vertical direction is 140°C at 35 m away from the fire, and 88°C at 72 m away from the fire. When the fire source power further increases to 80 MW, the highest temperature in the vertical direction is 175°C at 35 m away from the fire, and 105°C at 72 m away from the fire.

Under the 80 MW fire source power condition, when the exhaust gas flow rate is increased to 50 m^3/s, the highest temperature in the vertical direction is 167°C at 35 m away from the fire, and 103°C at 72 m away from the fire. With an exhaust gas flow rate of 60 m^3/s, the highest temperature in the vertical direction is 183°C at 35 m away from the fire, and 108°C at 72 m away from the fire. Except for the 80 MW condition, the highest temperature in the vertical direction is minimally affected by an increase in the exhaust gas flow rate.

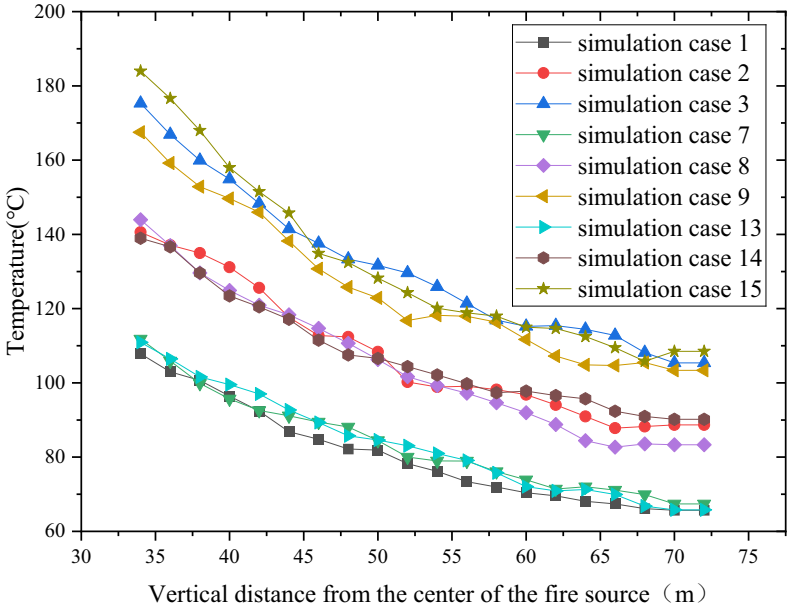

Fig. 5. Vertical temperature rise of fire source point A ceiling

6 Conclusions

At fire source point A, the longitudinal temperature rise of the roof exhibites a downward trend under different simulation cases. The maximum longitudinal temperature rise away from the fire source center is relatively low, while the highest temperature rise directly above the fire source reaches its peak. Additionally, the highest temperature rise at both ends of the fire origin displays a symmetrical shape. Under the same smoke exhaust volume conditions, an increase in fire source power results in an escalation of the maximum temperature elevation of the roof. Under the same fire source power, the impact of varying smoke exhaust volume on the Maximum temperature elevation of the roof is relatively minor.

Under the same fire source power, the height of the flue gas layer slightly decreases with the escalating smoke exhaust volume, but the downward trend is minor. Conversely, with a constant smoke exhaust volume, the smoke layer height increases with the fire source power, although the difference in height is negligible during the late stage of the fire. The variation trend of the smoke layer height at fire source point B is similar to that at fire source point A. However, the difference lies in the faster change in smoke layer height before 300 s, indicating a greater fire hazard.

In the observation of the vertical temperature rise in the ceiling at fire source point A, the temperature decreases exponentially with the increase in vertical distance from the center of the fire source, with the lowest temperature at the highest point. Under the condition of 80 MW fire source power, the vertical temperature rise in the ceiling is significantly influenced by an escalation in smoke exhaust volume. However, under other fire source power conditions, a rise in the volume of smoke exhaust does not produce a noticeable change in the vertical temperature rise.

The above are the relevant conclusions obtained from this simulation, but there are also some shortcomings in this article, such as the simulation process did not involve the characteristics of smoke under conditions of dual fire sources or multiple fire sources. In addition, when the power of the fire source is high, the thickness of the smoke layer will rapidly decrease in a short period of time, seriously threatening the evacuation and firefighting rescue work of personnel. Therefore, it is possible to consider installing ventilation equipment at both ends of the factory building and using mechanical smoke exhaust to improve the smoke situation effectively.

Acknowledgments

This work was financially supported by Research and Development Project of China Electric Power Research Institute (GC84-23-005).

References

1. Zhang, H. H., Zhang, S.C., Zhu, Z.Y. Experimental study on the maximum temperature rise of smoke in key smoke exhaust tunnel fires [J]. Fire Science and Technology, 2023,42 (08): 1067-1073. https://www.xfkj.com.cn/CN/.
2. Alpert, R. L. Calculation of response time of ceiling-mounted fire detectors [J]. Fire Technology, 1972.DOI:10.1007/BF02590543.
3. Li W. T. Numerical simulation study on cable fires in comprehensive pipe trenches [D] Beijing: Capital University of Economics and Trade, 2012. kns.cnki.net.
4. CHOW, W. K. Simulation of tunnel fires using a zone model [J]. Tunnelling and Underground Space Technology, 1996, 11(2):221-36. DOI:10.1016/0886-7798(96)00012-0.
5. Liu, Z.Y., Wang, X., Ran, H.N. Research on the smoke spread law of tunnel fires under dual fire source conditions of different heights [C] Collection of Fire Science and Technology Papers of the Academic Work Committee of the China Fire Protection Association (2023) - Basic Explosion Theory of Fire. China Petrochemical Press, 2023:4. DOI: 10.26914/c.cnkihy.2023.051979.
6. Xu, C. G. Research on the smoke diffusion law of tunnel dual fire source fire under longitudinal ventilation [D]. Anhui University of Science and Technology, 2023. DOI: 10.26918/d.cnki.ghngc.2023.000443.
7. Ren, F., Shi, C., Li, J. Numerical study on the flow characteristics and smoke temperature evolution under double fires condition with a metro train in tunnel[J]. Tunnelling and Underground Space Technology, 114. DOI: 10.1016/J.TUST.2021.103943.
8. Zhang, T, H. Study on temperature decay characteristics of fire smoke backflow layer in tunnels with wide-shallow cross-section[J]. Tunnelling and Underground Space Technology, 112. DOI:10.1016/J. TUST.2021.103874.
9. Xu, C, G. Research on the smoke diffusion law of tunnel dual fire source fire under longitudinal ventilation [D]. Anhui University of Science and Technology, 2023.000443. DOI: 10.26918/d.cnki.ghngc.2023.000443.
10. Cong, W. Fire smoke spread and characteristic parameter evolution in double narrow confined spaces of subway tunnels [D]. University of Science and Technology of China, 2022.000319. DOI: 10.27517/d.cnki.gzkju.2022.000319.
11. Z, W., Sun, C. P., Ma, W. H. Comparison of smoke exhaust effects between roof and lateral mechanical ventilation in tunnels [J]. Fire Science and Technology, 2021,40 (05): 639-643. https://www.xfkj.com.cn/CN/Y2021/V40/I5/639.
12. Liu C, T, X., Zhong, M. Full scale experimental study on fire-induced smoke propagation in large underground plant of hydropower station[J]. Tunnelling and Underground Space Technology, 2020, 103:103447. DOI: 10.1016/j.tust.2020.103447.
13. Zhang, G. C. Fire smoke diffusion and ventilation control based on hydroelectric power station traffic tunnels [D]. Xi'an University of Architecture and Technology, 2021.000951. DOI: 10.27393/d.cnki.gxazu.2021.000951.
14. Floyd, J. E., Forney, G. P. Fire Dynamics Simulator (Version 3) User's Guide[J]. 2002. https://www.doc88.com/p-38139035924277.html.
15. Zhu, J. A study on the influence of the arrangement of lateral smoke exhaust ports in tunnels on the characteristics of fire smoke movement [D]. Central South University, 2022.001317. DOI: 10.27661/d.cnki.gzhnu.2022.001317.